Int. J. Heat Mass Transfer. Vol. 33, No. 12, pp. 2683–2699, 1990
Printed in Great Britain

0017–9310/90 $3.00 + 0.00

Optimal synthesis of heat-and-power systems: the operating line method

EDUARDO O. PAVANI,† PÍO A. AGUIRRE† and HORACIO A. IRAZOQUI‡
Process Design, Optimization and Simulation Group, Instituto de Desarrollo Tecnológico para la Industria Química (INTEC), CONICET–UNL, Casilla de Correo No. 91, 3000 Santa Fe, República Argentina

(*Received* 13 *July* 1989 *and in final form* 6 *February* 1990)

Abstract—The physical and mathematical models on which the operating line method (OLM) (H. A. Irazoqui, *Chem. Engng Sci.* **41**, 1243–1255 (1986); P. A. Aguirre, E. O. Pavani and H. A. Irazoqui, *Chem. Engng Sci.* **44**, 803–816 (1989)) for the optimal synthesis of heat-and-power systems is built, are discussed in depth. These models include the heat exchange 'modes' allowed and the general features of the type of solution sought in order to reach an optimal scheme for the total energy systems in chemical plants. A thorough development of the mathematical technique used to tackle the optimization problem is also made. This development comprises the derivation of the necessary and sufficient conditions for optimality.

1. INTRODUCTION

IN THREE previous papers [1–3] (from now on quoted as Papers I, II and III, respectively), the operating line method (OLM) was proposed for the optimal synthesis of the heat-and-power cogeneration systems (HAPCS) for chemical processes with dominant power load.

The OLM is aimed at generating structures and operating conditions that bring the total steam utility consumption of the HAPCS, Q_v, to a minimum for each value of the total area of heat exchangers, A_E. Q_v is the amount of heat drawn from the hot utility, which is necessary to cover the process heat-and-power demand.

In Paper I, the physical model on which the method is based was presented. There, a brief outline of the mathematical formulation of the optimization problem and of the solution technique adopted was also made. In a first step those heat-and-power integration problems were considered in which only one steam level is available. The concept of operating line (OL) was central to the mathematical model for the derivation of the necessary conditions for optimality and for the application of the synthesis method to different situations. An important result was the identification of an *optimality region*, in which the corresponding OL has to be included so as to insure optimality.

In Paper II the OLM and the pinch design method [4] were compared on physical grounds, but special attention was given to applications. The results obtained showed that the hot utility usage predicted with the OLM was smaller than the one calculated with the Pinch design method for the same total power demand, when results were compared on the basis of the same value of A_E [2].

In Paper III the thermodynamic meaning of the optimality region was uncovered. Moreover, the extension of the OLM for the optimal synthesis devised in Paper I, to the more general case of multiple steam levels was also made. An interesting feature of the optimal solution for multiple steam level problems is that integration gaps arise.

Until now, the physical and mathematical model on which the OLM is based have not been presented together with a thorough discussion of the mathematical technique used to tackle the optimization problem. In previous communications, applications were stressed over discussion of mathematical procedures. This might handicap the full understanding of the method and the possibility of its extension to synthesis problems in which other kinds of transfer processes are present.

In this work, the OLM will be presented, with special emphasis made on physical and mathematical aspects. The thermodynamic model on which the method is built will be analyzed first. Then, the mathematical and physical models of the system including the 'modes' of exchange allowed and the general features of the type of solution sought will be discussed in depth. The variational technique adopted to solve the optimization problems will be reviewed. Necessary and sufficient conditions for optimality will also be analyzed. Finally, the mathematical features of the optimal solution and its physical interpretation will be discussed.

In order to gain simplicity, only problems with a single steam level will be considered. The conclusions

† Fellow of the National Research Council of Argentina (CONICET).

‡ Member of CONICET's Scientific and Technological Research Staff and Professor at the Universidad Nacional del Litoral (UNL). To whom correspondence should be addressed.

NOMENCLATURE

A_E total area of heat exchangers [m^2]
a ordinate at the origin of an OL [K]
E generalized function defined by equation (4) [dimensionless]
G objective function defined by equation (1) [kW]
H enthalpy flow [kW]
J functional defined by equation (34a) [kW K^{-1}]
LW lost work [kW]
P slope of the optimal OL [dimensionless]
Q heat exchanged per unit time [kW]
R generalized function defined by equations (19) [kW]
S entropy flow [kW K^{-1}]
T absolute temperature of a hot stream [K]
T_{int} ordinate of the intersection point between the optimal OL and the optimality region boundary for a given value of λ [K]
T_0 absolute temperature of the cold utility [K]
T_t derivative function of an OL [dimensionless]
T_v absolute temperature of the hot utility [K]
$\bar{T}$ modified absolute temperature [K]
$\bar{T}_{int}$ modified absolute temperature corresponding to the intersection point between the optimal OL and the optimality region boundary for a given value of λ [K]
t absolute temperature of a cold stream [K]
t_{int} abscissa of the intersection point between the optimal OL and the optimality region boundary for a given value of λ [K]
t_{LM} logarithm mean temperature between t_i and t_{i+1} [K]
U overall transfer coefficient [kW K^{-1} m^{-2}]
W hot stream heat capacity flow rate [kW K^{-1}].

Greek symbols

α positive value [dimensionless]
γ maximum energy recovery per unit area of heat exchangers [kW m^{-2}]
ε small positive quantity [dimensionless]
ζ arbitrary piece-wise constant function [K]
η global efficiency of an HAPCS [dimensionless]
θ step function [dimensionless]
Θ rectangular function [dimensionless]
κ constant value used in equation (2) and defined in Paper I [kW K^{-1}]
λ Lagrange multiplier [kW K^{-1} m^{-2}]
ξ Weierstrass function defined by equation (60) [kW K^{-1}]
σ rate of internal generation of entropy [kW K^{-1}]
σ^* combined function defined by equation (3) [kW K^{-1}]
σ_0^* constant defined by integrating equation (26) [kW K^{-1}]
τ_{CS} power generated by PGCs that operate between hot utility and unmatched cold process streams [kW]
τ_{HS} power generated by PGCs that operate between unmatched hot process streams and cold utility [kW]
Φ generalized function defined by equation (19b) [kW K^{-1}]
ω cold stream heat capacity flow rate [kW K^{-1}].

Subscripts

c properties associated with the CCS
E contribution due to the thermal exchange between composite streams
h properties associated with the HCS
i stream or temperature interval related to CS
j stream or temperature interval related to HS
v contribution due to thermal exchange with the hot utility.

Superscripts

i temperature interval related to CS
j temperature interval related to HS
* heat capacity flow rate of a branched composite stream matched according to an OL against the other composite stream.

Abbreviations

CCS cold composite stream
CS cold process streams
HAPCS heat-and-power cogeneration system
HCS hot composite stream
HEN heat exchanger network
HP high pressure
HS hot process streams
OL operating line
OLM operating line method
PGC power-generating cycle
SA-PGC stand-alone power-generating cycle.

as well as the mathematical technique for solving the problem, can be easily extended to more general cases in which several steam levels are available.

2. THE THERMODYNAMIC MODEL, ASSUMPTIONS AND CONSTRAINTS

In an HAPCS, hot process streams (HS) exchange heat with cold process streams (CS) in a subsystem comprising a heat exchange network (HEN). Each HEN corresponds to a particular pairing policy between HS and CS.

Heat exchange between process streams is not always feasible. In addition, the amount of heat absorbed by CS is seldom in balance with the amount of heat delivered by HS. As a consequence of this, local heat sinks and sources remain after a particular matching policy between process streams has been implemented. Efficient power generation can be achieved by coupling power-generating cycles (PGCs) to these heat sinks and sources.

In an HAPCS, process heat sources deliver heat to PGCs which, in turn, reject heat to the cooling water of temperature T_0. Heat sinks, on the other hand, take heat from the heat discharge of PGCs which use the high pressure (HP) steam of temperature T_v, as the heat source. When additional power is required, it must be generated by a 'stand-alone' PGC (SA-PGC) operating between the temperature of the HP steam and that of the cooling water. This is a typical situation in dominant power load cases. For more details the reader is referred to Papers I and II. A sketch of the thermodynamic system comprising the HAPCS and the SA-PGC is shown in Fig. 1.

The OLM considers heat integration with coupled power generation as a unique, non-separable problem. From the beginning, heat integration between process streams is influenced by the fact that the remaining local heat sources and sinks will be, in principle, exploited to achieve efficient power generation. In this respect it is important to remark that the maximum amount of power that can be generated by coupling PGCs to process heat sinks sources depends on both the magnitude of the interaction and the temperature at which it occurs.

The thermodynamic model on which the OLM is based can be formulated in terms of composite streams. The cold composite stream (CCS) is a single, effective cold stream the heat capacity flow rate (i.e. mass flow times the specific heat) of which is assumed to be piece-wise constant. For a given temperature, the heat capacity flow rate of the CCS is computed by adding up the heat capacity flow rate of the individual CS with the same temperature. The hot composite stream (HCS) is computed in an analogous way.

The model is constrained so that, for a given stream pairing policy, heat exchange between the HCS and CCS, whenever it is feasible, is mandatory, maximizing the amount of heat exchanged so as to completely satisfy one of the composite streams. The HCS can also deliver excess heat to PGCs. The energy required by the CCS in excess over the amount of heat exchanged with the HCS will be provisionally considered as being supplied by direct heating using the auxiliary hot utility.

Heat exchange between the HCS and PGCs, and between the CCS and the hot utility, are both considered 'supplementary modes'. They only become 'active' (one mode at a time) to satisfy eventual heating or cooling local needs remaining after local possibilities for heat exchange between integrated process streams have been exhausted. These constraints, characterizing the type of solution sought, have been systematically incorporated in the formulation of the optimization problem, as will be outlined in Section 4. Figure 2 shows a scheme of the thermodynamic model just described.

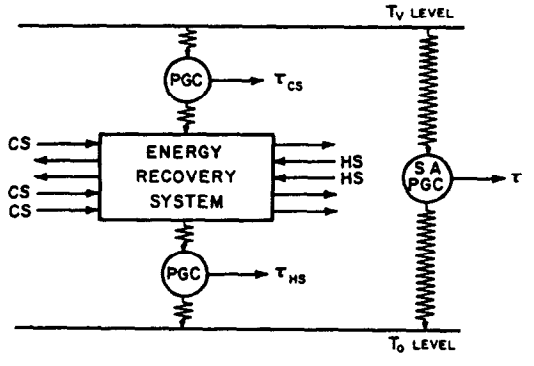

FIG. 1. Sketch of the thermodynamic system comprising the HAPCS and the SA-PGC.

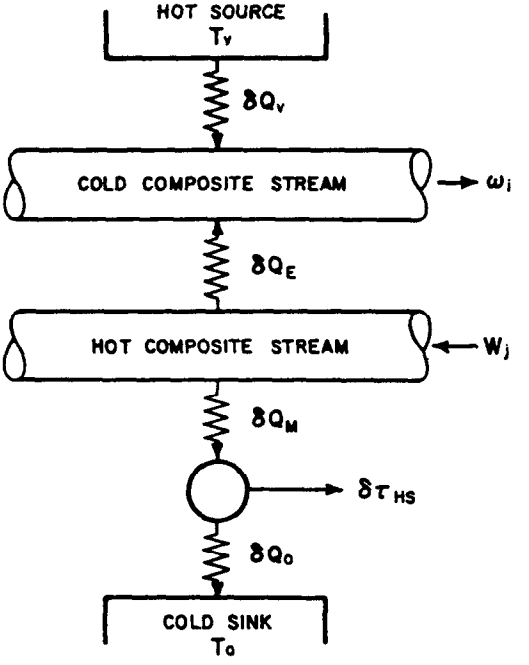

FIG. 2. Elementary exchanges along degrees of freedom allowed in the thermodynamic model.

This model allows a synthesis procedure to be devised so that a practical solution with convenient general features is obtained. Hence the solution sought is not the most efficient one in purely abstract thermodynamic terms. Moreover, it gives priority to the use of HP steam to generate shaft power by means of an SA-PGC over its use on PGCs discharging heat upon process sinks. This bias is introduced in the formulation by assigning the lowest possible value to the efficiency of PGCs operating in the latter kind of arrangement. This limiting situation in which the efficiency is zero, corresponds to the direct heating of CS by means of auxiliary steam. After the optimal solution is obtained, this restriction is removed by supplying heat to process sinks by means of the heat discharge of practical PGCs. This, by no means changes the optimum reached because, as it will be seen, the objective function value is not altered by this evolution.

The rationale for this strategy stems from the type of solution sought in which heat exchange between process streams has priority over power generation by means of PGCs thermally coupled to process heat sinks/sources. This has to be so because, the maximum efficiency attainable with coupled power generation is always smaller than that of an SA-PGC, when both efficiencies are compared as the ratio of the shaft power produced in each case, over the same total amount of heat supplied by the auxiliary heat source. Therefore, without the constraint making heat exchange mandatory, the most efficient solution will always be the one that forbids energy degrading heat integration of process streams.

3. THE OBJECTIVE FUNCTION

Heat recovery through stream thermal integration and through coupled power generation have competing trends. An appropriate objective function, G, able to evaluate the energy performance of an HAPCS subjected to the constraints described in the previous section, has already been derived in Paper I.

The optimal synthesis problem can be formulated in terms of G. If T_v is the absolute temperature of the HP stream level, which is assumed to have been fixed beforehand, and T_0 is that of the cold utility, then the OLM is aimed at finding the HAPCS that maximizes the objective function

$$G = Q_E\left(\frac{T_v - T_0}{T_v}\right) + \tau_{HS} \qquad (1)$$

for each value of the total transfer area of heat exchangers, A_E.

The objective function G is made up of two terms. The first one ponders the two aspects of energy savings due to heat recovery: the amount of energy, Q_E, computed as energy savings in the auxiliary heat source, and its quality as measured by the Carnot efficiency $((T_v - T_0)/T_v)$. The second term in G, τ_{HS}, represents the maximum amount of work obtainable by coupling PGCs to local process heat sources.

It is obvious that different pairs of values can be assigned to the two terms of equation (1), all yielding the same value of G. The model is constrained so that the optimal pairing policy that makes G maximum for a given value of the total exchange area, A_E, also makes maximum the ratio Q_E/τ_{HS}. Hence, heat recovery through thermal integration has been given priority over power generation from process heat sources. Additional power needs must be satisfied by an SA-PGC as is the situation in dominant power load cases. However, every HAPCS synthesis problem can be considered, at least initially, as belonging to that class. This is so because the optimal solution obtained with the OLM for dominant power load cases can always be optimally evolved toward alternative ones showing the same value of Q_E, smaller size of the total area of heat exchangers, A_E, and smaller power output (see Paper I).

For each given value of A_E, the optimal solution will render the maximum value of the ratio $\gamma = G_i/A_E$, which measures the energy savings per unit of heat exchange area. This will always represent the best alternative when compared with other solutions on the basis of equal values of A_E.

An economic evaluation of optimal solutions, each one corresponding to a different value of A_E, will single out the most profitable one. However, it must be stressed that different economic circumstances can only shift the interest from one optimal solution relating to a given value of A_E to another involving a different size of the exchange area, since the optimality criterion on which the solutions are built are permanent goals, i.e. maximum energy recovery per unit area of heat exchangers, as measured by γ, for each A_E value. At this point, the notion can be advanced that the trend of γ is also the trend of the ratio of the economic benefit obtained with the HAPCS, related to G, to the capital costs, related to A_E.

In short, each optimal solution will show:

(i) The maximum value of G for the corresponding value of A_E.

(ii) The maximum value of Q_E, provided that condition (i) has already been met.

Therefore, generation of shaft power using the HCS as the heat source, although subsidiary to thermal energy recovery, is also a maximum.

As was already pointed out, the two terms in G have competing trends. Any quantity of heat exchanged between HS and CS diminishes the maximum amount of work obtainable through thermal coupling between PGCs and process streams. Therefore, there is a trade-off between heat integration and coupled power generation. This precludes the possibility of finding the maximum for the objective function by sequentially looking for the maximum of one term at a time.

In Paper I it has been shown that for the proposed

model, the rate of internal generation of entropy [5], σ, is related to G through

$$\sigma = \kappa - \frac{G}{T_0} \tag{2}$$

where κ is a constant whenever inlet and outlet temperature of process streams are given. Therefore, seeking a maximum for G is equivalent to seeking a minimum for σ, with the constraints discussed above. For convenience, the mathematical statement of the optimization problem will be made in terms of σ rather than G.

As can be concluded from (i), an optimal solution corresponds to a constrained maximum of G (or minimum of σ) subjected to the condition $A_E = A_0$, with A_0 a constant value. As is well known, this is equivalent to the minimum of the combined objective function

$$\sigma^* = \sigma + \lambda A_E \tag{3}$$

where λ is a Lagrange multiplier (see p. 210 of ref. [6]).

4. THE MATHEMATICAL MODEL

In this section, the mathematical model for an HAPCS proposed in Paper I will be reviewed. This mathematical model is cast into a form apt for the application of variational calculus. This was done by expressing σ^*, defined by equation (3), as a functional of the matching policy of process streams. This functional should also contain information regarding each particular problem under consideration, as inlet and outlet temperatures of process streams and their heat capacity flow rates. The exchange modes that are allowed to be 'active' in the model and the priority given to heat exchange over the utility usage will also be introduced into the functional through an appropriate formulation.

4.1. *The exchange region and the total heat capacity flow rate*

Part of the description of each particular problem is introduced in the formulation by the definition of the exchange region.

For the heat exchange process the exchange region is made up of all points on a t vs T plane for which heat exchange from an HCS of absolute temperature T to a CCS of absolute temperature t, is feasible. The mathematical expression of the condition that a pair (t, T) must satisfy to belong to the exchange region, must be established. In order to do this, feed and target temperatures (i.e. stream outlet temperatures) of original HS are organized in a decreasing order and designated by T_j; $j = 1, 2, \ldots$. Analogously, feed and target temperatures of original CS are organized in an increasing order and designated by T_i; $i = 1, 2, \ldots$. For each of these values of t_i (or T_j), at least one original CS (or HS) enters or leaves the system.

A function $E(t, T)$ is defined as

$$E(t, T) = \Theta_3(t, T) \sum_i \sum_j \Theta_1^{(i)}(t) \theta_2^{(j)}(T) \tag{4}$$

in which

$$\Theta_1^{(i)}(t) = \theta[\omega_i(t - t_i) - \varepsilon]\theta[\omega_i(t_{i+1} - t) - \varepsilon] \tag{5}$$

$$\Theta_2^{(j)}(T) = \theta[W_j(T - T_{j+1}) - \varepsilon]\theta[W_j(T_j - T) - \varepsilon] \tag{6}$$

and

$$\Theta_3(t, T) = \theta(T - t). \tag{7}$$

In equations (5)–(7), $\theta(x)$ is the step (Heaviside) function [7], ω_i and W_j are the total heat capacity flow rates of the CCS and the HCS inside subinterval i and j, respectively, and ε is a small positive quantity. For each point (t, T) inside the exchange region. it holds that

$$E(t, T) = 1. \tag{8}$$

An immediate consequence of these definitions is that the total heat capacity flow rate of the CCS and the HCS are given by

$$\omega(t) = \sum_i \theta_1^{(i)}(t) \omega_i \tag{9}$$

and

$$W(T) = \sum_j \Theta_2^{(j)}(T) W_j \tag{10}$$

respectively.

Finally, the (i, j)-exchange subregion is made up of all (t, T) pairs such that $t_i < t < t_{i+1}$ and $T_{j+1} < T < T_j$.

4.2. *The operating line. Maximum local exchange constraint*

Another key element for the construction of the functional σ^* is the definition of the operating line. For the heat exchange process, an OL is a function $T = f(t)$ which establishes a matching policy between the CCS of temperature t and the HCS of temperature T, provided that (t, T) belongs to the exchange region.

When the CCS, whether exchanging heat with the HCS or not, increases its temperature by dt about t following a given OL $T = f(t)$, it requires an amount of heat given by

$$\delta Q_c = \omega(t)\, dt. \tag{11}$$

The amount of heat δQ_c can be supplied by the HCS of temperature $T = f(t)$ and by the steam utility of temperature T_v. The corresponding change in the temperature of the thermally integrated HCS for the given OL, is

$$dT = |T_t|\, dt \tag{12}$$

where the expression in bars is the absolute value of $T_t = df/dt$. Equation (12) holds both for co-current and counter-current pairing patterns and was written so that the amount of heat yielded by the HCS, expressed by

$$\delta Q_h = W(T)\,dT \tag{13}$$

is always a positive quantity.

As was pointed out in Section 2, the model is constrained so that when these changes in the temperature of the composite streams occur, the heat delivered by the HCS is first used to supply the CCS with the heat it demands up to the amount δQ_c. An eventual excess is then used to produce shaft power. The two situations that may arise are depicted in Fig. 3. Consequently, whenever

$$\delta Q_h < \delta Q_c; \quad E(t, T) = 1 \tag{14}$$

it must hold that

$$\delta Q_E = \delta Q_h \tag{15}$$

where $E(t, T) = 1$ stands for the fact that heat exchange between process streams is feasible. This situation is illustrated in Fig. 3(a).

On the other hand, when

$$\delta Q_h \geqslant \delta Q_c; \quad E(t, T) = 1 \tag{16}$$

it is required that

$$\delta Q_E = \delta Q_c. \tag{17}$$

This is the situation illustrated in Fig. 3(b).

In Paper I, all these constraints have been introduced at once by prescribing that the expression for the heat exchanged between the HCS and the CCS must be of the form

$$\delta Q_E = R(t, T, T_t)\,dt \tag{18}$$

in which

$$R(t, T, T_t) = \Theta_3(t, T)\sum_i \Theta_1^{(i)}(t)\sum_j \Theta_2^{(j)}(T)\Phi_{ij}(T_t) \tag{19a}$$

and

$$\Phi_{ij}(T_t) = [(\omega_i - W_j|T_t|)\theta(W_j|T_t| - \omega_i + \varepsilon) + W_j|T_t|]. \tag{19b}$$

The expression for $\Phi_{ij}(T_t)$ given by equation (19b) takes into account the possibility of either countercurrent heat exchange (in which $T_t > 0$) or co-current heat exchange (in which $T_t < 0$). The generalized function $\Phi_{ij}(T_t)$ has been constructed in a way such that δQ_E, as given by equation (18), reduces to either equation (15) under the conditions given by equation (14), or to equation (17) under the conditions described by equation (16).

With these definitions, the expression for the corresponding amount of heat to be supplied by the steam utility, δQ_v, for a given OL $T = f(t)$, becomes

$$\delta Q_v = [\omega(t) - R(t, T, T_t)]\,dt. \tag{20}$$

As in Paper I, the rate of internal generation of entropy can be expressed as a functional $\sigma\,[f]$ of the OL, incorporating the constraints discussed above. The same can be said as regards the total exchange area, which can be expressed as a functional $A_E[f]$. As a consequence, σ^* is also a functional of the OL.

The rate of internal generation of entropy corresponding to either case of Fig. 3 is given by the expression

$$\delta\sigma = \delta Q_v\left(\frac{1}{t} - \frac{1}{T_v}\right) + \delta Q_E\left(\frac{1}{t} - \frac{1}{T}\right) \tag{21}$$

provided that δQ_E and δQ_v are given by equations (18)

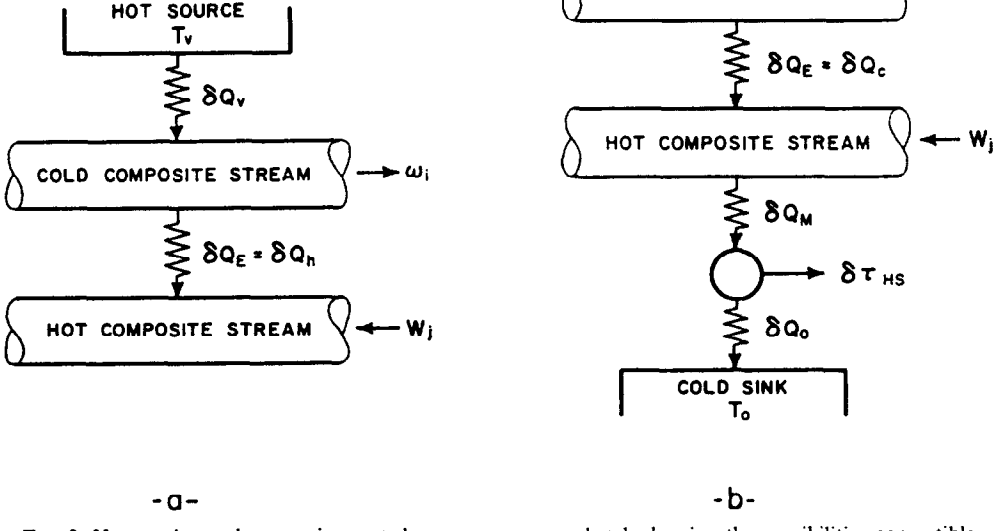

FIG. 3. Heat exchange between integrated process streams: sketch showing the possibilities compatible with the constraints imposed.

and (20), respectively. With the same assumptions, the corresponding heat exchange area involved is

$$\delta A_E = \frac{\delta Q_E}{U(T-t)} \tag{22}$$

where U is an overall transfer coefficient. The contribution to the value of σ^* of the elementary exchange can be expressed as

$$\delta\sigma^* = \delta\sigma + \lambda\delta A_E. \tag{23}$$

Combining equations (18) and (20)–(23) the following expression for $\delta\sigma^*$ is found:

$$\delta\sigma^* = \delta\sigma_0^* + R(t, T, T_t)\left[\left(\frac{1}{T_v} - \frac{1}{T}\right) + \frac{\lambda}{U}\frac{1}{(T-t)}\right]dt \tag{24}$$

where

$$\delta\sigma_0^* = \omega(t)\left[\frac{1}{t} - \frac{1}{T_v}\right]dt \tag{25}$$

which, in fact, amounts to

$$\delta\sigma_0^* = \delta S_c - \frac{1}{T_v}\delta H_c \tag{26}$$

where the elementary entropy change of the CCS is

$$\delta S_c = \frac{\omega(t)}{t}dt \tag{27}$$

and δH_c is the elementary change of enthalpy in the same composite stream given by

$$\delta H_c = \omega(t)\,dt. \tag{28}$$

The expression of σ^* as a functional of the OL $T = f(t)$, can be obtained by integrating equation (24) along the interval $0 < t < \infty$. The expression thus obtained is

$$\sigma^*[f;\lambda] = \sigma_0^* + \int_0^\infty R(t, T, T_t)\left[\left(\frac{1}{T_v} - \frac{1}{T}\right) + \frac{\lambda}{U}\frac{1}{(T-t)}\right]dt \tag{29}$$

where $\sigma^*[f;\lambda]$ stands for a functional the value of which depends on the particular choice made on the OL, $T = f(t)$, and on the value of λ. Besides, σ_0^* is a constant under the assumption that the inlet and outlet temperatures of every CS are given. It is important to remark that, although the integration performed on equation (24) is formally carried out over the entire interval $0 < t < \infty$, the integrand is zero outside the exchange region (i.e. for $E(t, T) = 0$).

A point has been reached in which the mathematical formulation of the problem is ripe for the application of variational calculus to seek for the optimal OL.

5. DISCUSSION OF THE MODEL

The model has been formulated in terms of composite streams, the total heat capacity flow rates of which are piece-wise constant functions of the temperature, as given by equations (9) and (10). Discontinuities in the total heat capacity flow rates occur at temperature values corresponding to those of streams entering or leaving the HEN.

It is usual to represent the cooling profile of an HCS and the heating profile of a CCS on an H vs T plane. These T–H diagrams, widely used in stream thermal integration problems [8], have piece-wise constant slopes given by

$$\frac{dT}{dH} = \frac{1}{W_j}; \quad T_{j+1} < T < T_j \tag{30a}$$

for the cooling profile of the HCS, and

$$\frac{dt}{dH} = \frac{1}{\omega_i}; \quad t_i < t < t_{i+1} \tag{30b}$$

for the heating profile of the CCS, respectively.

The overlap between the H-axis projection of the HCS cooling profile and that of the CCS heating profile on a T–H diagram, is a measure of the amount of heat that can be exchanged between process streams. A vertical line intersecting both profiles simultaneously, determines a pair (t, T) for which heat exchange between composite streams is feasible. The set of all (t, T) pairs satisfying this condition gives rise to a function $T = f(t)$ for each degree of overlapping between the H-axis projection of the cooling and heating profiles. The single valued function $T = f(t)$ is the operating line, which represents a particular pairing policy between process streams.

From these considerations it can be concluded that in this model the OL is a function with piece-wise constant slope on a t vs T plane.

Assuming that $T = f(t)$ is an OL (not necessarily optimal) with the general features just described, a modified temperature $\bar{T}$ given by

$$\bar{T} = T - \frac{\Delta T}{2} \tag{31a}$$

for the HCS, and by

$$\bar{T} = t + \frac{\Delta T}{2} \tag{31b}$$

for the CCS can be defined, where

$$\Delta T = T - t = f(t) - t. \tag{31c}$$

This change of variables from (H, T) into $(H, \bar{T})$, amounts to a downward shift of the HCS cooling profile by a variable quantity $\Delta T/2 = (f(t) - t)/2$, and to an upward shift of the CCS heating profile by the same amount. Accordingly, a contact point between the two profiles in a $\bar{T}$–H diagram means that their temperatures locally differ by ΔT and that heat exchange is still possible.

Both profiles in a $\bar{T}$–H diagram show breaking points (Fig. 4(a)), corresponding to sudden changes in their total heat capacity flow rates due to streams entering or leaving the HEN.

The $\bar{T}$–H diagram can be horizontally partitioned at those breaking points, giving rise to a series of temperature intervals along the vertical temperature scale. The total heat capacity flow rates of the HCS and the CCS are constant inside each of these $\bar{T}$ intervals. At the boundaries of each interval, at least one of the original streams enters or leaves the HEN.

The same partitioned $\bar{T}$–H diagram could have been obtained from a larger set of pseudostreams. This new set is made up of all pseudostreams generated by breaking up the original streams at every $\bar{T}$ interval boundary they encounter between their feed and target temperatures, thus generating an equivalent, larger set of streams. By construction, every pseudostream in the new set, whether hot or cold, covers the stretch of a single temperature interval. This allows each temperature interval in the $\bar{T}$–H diagram to be considered as separate from the rest.

Any of the two profiles inside a temperature interval can be horizontally shifted until a point of contact is established with the other profile in the same interval. The situation reached is that of maximum exchange between the HCS and the CCS in the interval for the given OL which, in turn, gives ΔT as a function of t through equation (31c). When this operation is repeated for every temperature interval, a situation like the one shown in Fig. 4(b) is reached. The overshoot of the CCS in a given interval, if it occurs, represents the minimum demand of external heating in the interval, whereas an eventual overshoot of the HCS represents the interval needs for external cooling.

The remaining question is whether the HCS and the CCS profiles in the interval are in a situation of exchanging heat obeying the given OL or not. If they do so, the temperature difference between them in the interval should satisfy equation (31c), which in terms of $\bar{T}$ can be written as

$$\Delta\bar{T} = 0. \tag{32}$$

In general, this condition is not satisfied at the interior of each temperature interval as illustrated in Fig. 4(b).

The condition given by equation (32) can be met by branching the composite stream corresponding to the overshooting profile so that the condition

$$\omega(\bar{T}) = W(\bar{T})T_t(\bar{T}) \tag{33}$$

holds for integrated streams in the interior of every temperature interval. The unmatched branch of the overshooting composite stream in each interval behaves as a process heat source or sink, depending on whether the branched composite stream is hot or cold, respectively (Fig. 4(d)).

The new construction, schematically shown in Fig. 4(c), guarantees that equation (32) is satisfied at every exchange situation. It is not until the above operations are performed that the particular OL chosen truly represents a stream pairing policy.

It is important to remark that the constraint of maximum local heat exchange, mandatory within the present model for any adopted OL, has been observed throughout the above operations. The results arrived at are summarized in Fig. 5 for a given, non-optimal, OL.

6. OPTIMIZATION PROCEDURE

6.1. *Derivation of necessary conditions*

For a given synthesis problem, it is assumed that the optimal OL is known and that the original streams have been broken up giving rise to an equivalent, though larger set of pseudostreams. Thus, a diagram

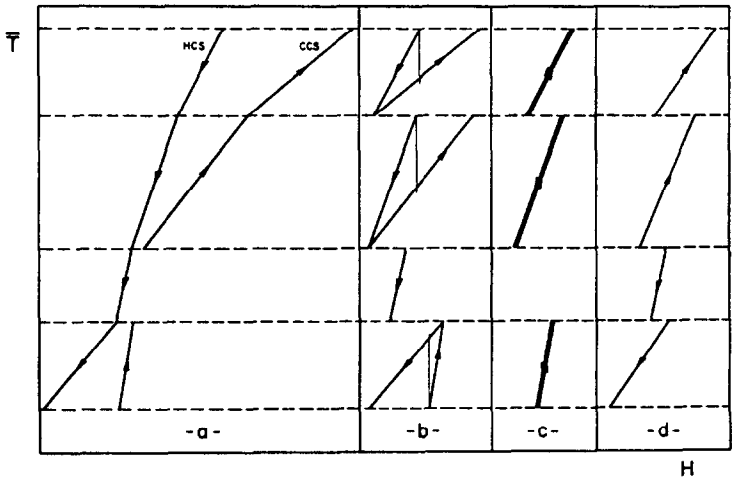

FIG. 4. Heating and cooling profiles in a $\bar{T}$–H diagram: (a) HCS and CCS profiles; (b) profiles at the relative position of maximum exchange between the pseudostreams for a given OL; (c) profiles for the integrated pseudostreams undergoing heat exchange along a given OL; (d) profile of umatched branch of the overshooting pseudostream split in each $\bar{T}$ interval.

like the one shown in Fig. 5 can be constructed, which is the starting point for the mathematical development leading to the solution of the optimization problem.

The optimal OL is the one that makes the functional σ^* of equation (29) attain its minimum for the chosen value of λ.

Since σ_0^* in equation (29) is a constant for each given problem, it is sufficient to consider the functional

$$J = \int_0^{\infty} F(t, T, T_t)\, dt \tag{34a}$$

where

$$F(t, T, T_t) = R(t, T, T_t)\left[\left(\frac{1}{T_v} - \frac{1}{T}\right) + \frac{\lambda}{U}\frac{1}{(T-t)}\right] \tag{34b}$$

instead of the expression given by equation (29), without loss of generality.

In order to identify the optimal (minimal) OL, a variational technique will be used. For the purpose of deriving necessary conditions, the variations considered may be specialized as much as convenient (see p. 15 of ref. [6]).

The portion of optimal OL lying inside a generic (i, j) exchange subregion on a t vs T diagram is considered, like the one shown in Fig. 6. A variation $\alpha\zeta(t)$, where α is a positive value, is chosen which satisfies the following conditions:

(i) It belongs to the same class of functions as the optimal OL does, i.e. its slope is piece-wise constant.

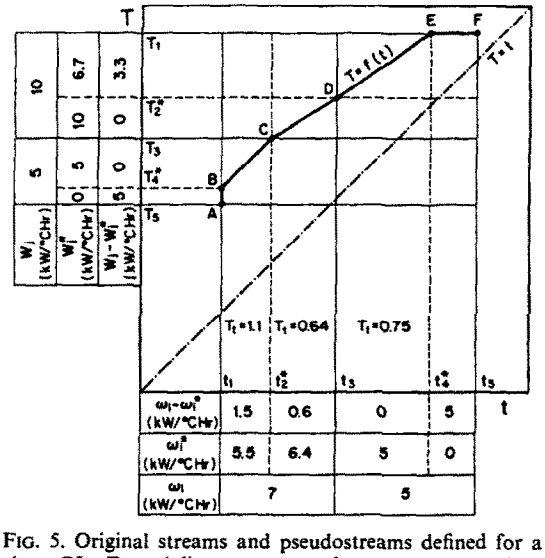

FIG. 5. Original streams and pseudostreams defined for a given OL. Dotted lines represent the temperature values (denoted by T_j^* and t_i^*) at which the original streams have been cut to generate the set of pseudostreams. These values correspond to the OL breaking points B, C, D and E. Heat capacity flow rates with asterisks represent effective heat capacity flow rates of the composite stream matched according to the OL against the other one.

(ii) At opposite corners of the generic (i, j) subregion it must hold that

$$\zeta(t_i) = \zeta(t_{i+1}) = 0. \tag{35}$$

Moreover, $\zeta(t) = 0$ outside the (i, j) subregion which, in turn, is any subregion among all the exchange subregions.

A variation of this class is shown in Fig. 6. The total variation of the integral J is

$$\Delta J = \int_0^{x} [F(t, T+\alpha\zeta, T_t+\alpha\zeta') - F(t, T, T_t)]\, dt \tag{36}$$

which can also be written as

$$\Delta J = \int_{t_i}^{t^*-0} [F(t, T+\alpha\zeta, T_t+\alpha\zeta') - F(t, T, T_t)]\, dt + \int_{t^*+0}^{t_{i+1}} [F(t, T+\alpha\zeta, T_t+\alpha\zeta') - F(t, T, T_t)]\, dt. \tag{37}$$

Assuming that α is a constant the absolute value of which is taken so small that Taylor's formula can be applied to the integrands in equation (37), then

$$\Delta J \simeq \delta J = \alpha\left\{\int_{t_i}^{t^*-0} (F_T\zeta + F_{T_t}\zeta')\, dt + \int_{t^*+0}^{t_{i+1}} (F_T\zeta + F_{T_t}\zeta')\, dt\right\} \tag{38}$$

where δJ stands for the first variation of J, $F_T = \partial F/\partial T$ and $F_{T_t} = \partial F/\partial T_t$.

Integrating by parts the second term in each integrand of equation (38), it becomes

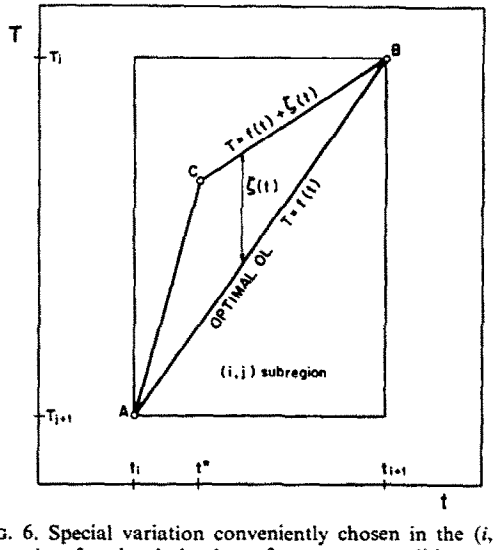

FIG. 6. Special variation conveniently chosen in the (i, j) subregion for the derivation of necessary conditions and $\alpha = 1$. At the subregion opposite corners it holds that $\zeta(t_i) = \zeta(t_i+1) = 0$.

$$\delta J = \alpha\left\{[\zeta F_T]_{t_i}^{t^*-0} + \int_{t_i}^{t^*-0} \zeta\left(F_T - \frac{\mathrm{d}}{\mathrm{d}t}F_{T_i}\right)\mathrm{d}t + [\zeta F_T]_{t^*+0}^{t_{i+1}} + \int_{t^*+0}^{t_{i+1}} \zeta\left(F_T - \frac{\mathrm{d}}{\mathrm{d}t}F_{T_i}\right)\mathrm{d}t\right\}. \quad (39)$$

Since ζ vanishes at t_i and at t_{i+1}, this leads to the condition that for an extremum it is necessary that

$$F_T - \frac{\mathrm{d}}{\mathrm{d}t}F_{T_i} = 0 \quad (40a)$$

in the interior of the generic (i, j) subregion, together with

$$\zeta(t^*-0)F_{T_i}(t^*-0) = \zeta(t^*+0)F_{T_i}(t^*+0) \quad (40b)$$

for $t_i < t^* < t_{i+1}$.

Since the optimal OL, provided that it exists, has a constant slope inside each subregion, and taking into account that $\zeta(t^*-0) = \zeta(t^*+0)$ due to the type of variation chosen, then equation (40b) is satisfied for the admissible class of solutions.

Inside the interval (t_i, t_{i+1}), and for an OL with piece-wise constant slope given by

$$T(t) = a_{ij} + P_{ij}t; \quad T > t \quad (41)$$

where a_{ij} and P_{ij} are constant values, equation (40a) becomes

$$\left[\frac{1}{T^2} - \frac{\lambda}{U}\frac{1}{(T-t)^2}\right]\omega_i\theta(W_j|P_{ij}| - \omega_i + \varepsilon) - \frac{\lambda}{U}\frac{1}{(T-t)^2}W_j \operatorname{sign}(P_{ij})[1 - \theta(W_j|P_{ij}| - \omega_i + \varepsilon)] = 0 \quad (42)$$

as shown in the Appendix.

When the inequality

$$W_j|P_{ij}| < \omega_i \quad (43a)$$

holds, then

$$\theta(W_j|P_{ij}| - \omega_i + \varepsilon) = 0 \quad (43b)$$

and equation (42) reduces to

$$\frac{\lambda}{U}\frac{1}{(T-t)^2}W_j = 0 \quad (43c)$$

which for $\lambda \neq 0$ cannot be satisfied by any straight OL.

On the other hand, for

$$W_j|P_{ij}| \geqslant \omega_i \quad (44a)$$

equation (42) becomes

$$\left[\frac{1}{T^2} - \frac{\lambda}{U}\frac{1}{(T-t)^2}\right]\omega_i = 0 \quad (44b)$$

which corresponds to an optimal OL given by

$$T(t) = \frac{1}{1 - \sqrt{\left(\frac{\lambda}{U}\right)}}t. \quad (45)$$

Comparing equation (41) with equation (45), it can be concluded that

$$a_{ij} = 0 \quad (46a)$$

and

$$T_i = \frac{1}{1 - \sqrt{\left(\frac{\lambda}{U}\right)}} = P \quad (46b)$$

regardless of the subregion considered, since λ/U is a constant.

From equation (45) it follows that the range of $P(\lambda)$ is

$$1 < \frac{\omega_i}{W_j} < P < \infty \quad (47)$$

which is a consequence of T and t being absolute temperatures. These results are valid for all (i, j) subregions.

6.2. *Interpretation of necessary conditions*

There are two contributions to σ, namely, the one associated to heat exchange between integrated process streams, σ_E, and the one associated to the direct heating of the excess cold streams by means of the steam utility, σ_v. For OLs which satisfy equation (45), these contributions in the (i, j) subregion are given by

$$\sigma_E = \Phi_{ij}(P)\left(\frac{P-1}{P}\right)\ln\left(\frac{t_{i+1}}{t_i}\right) \quad (48a)$$

and

$$\sigma_v = [\omega_i - \Phi_{ij}(P)]\left(1 - \frac{t_{LM}}{T_v}\right)\ln\left(\frac{t_{i-1}}{t_i}\right) \quad (48b)$$

respectively, where $t_{LM} = (t_{i+1} - t_i)/\ln(t_{i-1}/t_i)$.

The area of heat exchangers for the same subregion is

$$A_E = \frac{1}{U}\frac{\Phi_{ij}(P)}{(P-1)}\ln\left(\frac{t_{i+1}}{t_i}\right). \quad (49)$$

It is important to remark that an OL given by equation (45) satisfies the necessary conditions for a local minimum only when $W_jP \geqslant \omega_i$.

A situation in which $W_jP < \omega_i$ can be thought of as having been reached by continuously increasing ω_i, starting from an initial value which is smaller than the product W_jP. For a fixed value of the slope of the

optimal OL, $P = P_1$, this initial point can be any point A′ in the segment AB of Fig. 7.

As long as $W_j P_1 \geqslant \omega_i$, the chosen OL satisfies the necessary conditions for a local minimum. In addition

$$\sigma_E = \omega_i \left(\frac{P_1 - 1}{P_1}\right) \ln\left(\frac{t_{i+1}}{t_i}\right) \tag{50a}$$

$$\sigma_v = 0 \tag{50b}$$

and

$$A_E = \frac{1}{U} \frac{\omega_i}{(P_1 - 1)} \ln\left(\frac{t_{i+1}}{t_i}\right). \tag{50c}$$

Along A′B, the ratio (σ/A_E) maintains its optimum value corresponding to $P = P_1$

$$\left(\frac{\sigma}{A_E}\right)_{opt} = U \frac{(P_1 - 1)^2}{P_1}; \quad W_j P_1 \geqslant \omega_i \tag{51}$$

irrespective of the value of ω_i. This situation lasts until the condition $\omega_i = \omega_i^* = W_j P_1$ is reached. This happens at point B of Fig. 7.

From beyond point B, both σ_E and A_E remain constant, maintaining each one the largest value attained, given by

$$\sigma_E = W_j (P_1 - 1) \ln\left(\frac{t_{i+1}}{t_i}\right) \tag{52a}$$

and

$$A_E = W_j \frac{P_1}{U(P_1 - 1)} \ln\left(\frac{t_{i+1}}{t_i}\right) \tag{52b}$$

respectively, as can be concluded from equations (48a) and (49).

On the other hand, the contribution σ_v is equal to zero along A′B, but increases linearly with ω_i beyond point B, according to

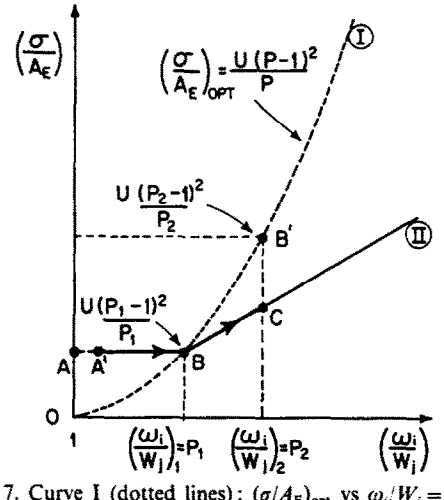

FIG. 7. Curve I (dotted lines): $(\sigma/A_E)_{opt}$ vs $\omega_i/W_j = P$, as given by equation (51). Curve II: trajectory with constant A_E, representing all (σ/A_E) values obtained by increasing ω_i starting from point A′, which represents an initial optimal solution for $P = P_1$. The product W_j/P_1 is kept constant.

$$\sigma_v = [\omega_i - P_1 W_j] \left(1 - \frac{t_{LM}}{T_v}\right) \ln\left(\frac{t_{i+1}}{t_i}\right) \tag{52c}$$

until the actual value of ω_i is reached at point C of Fig. 7. The trend of σ/A_E as a function of ω_i/W_j, with P and W_j kept constant, is shown as the trajectory A′BC.

Curve I of Fig. 7, containing the breaking points of all possible trajectories, is the representation of $(\sigma/A_E)_{opt}$ as a function of P, given by equation (51) for $1 < \omega_i/W_j = P < \infty$.

Considering

$$\left.\frac{\partial(\sigma/A_E)}{\partial(\omega_i/W_j)}\right|_{(W_j P_1)} = U \frac{(P_1 - 1)}{P_1} \left[1 - \frac{t_{LM}}{T_v}\right] \tag{53}$$

which is valid for $\omega_i/W_j > P_1$, with $0 < (1 - t_{LM}/T_v) < 1$, and

$$\left.\frac{\partial(\sigma/A_E)_{opt}}{\partial(\omega_i/W_j)}\right|_{(\omega_i^* = W_j P_1)} = \frac{U(P_1 - 1)}{P_1} \left[\frac{P_1 + 1}{P_1}\right] \tag{54}$$

with $1 < [(P_1 + 1)/P_1] < 2$, it can be concluded that

$$0 < \left.\frac{\partial(\sigma/A_E)}{\partial(\omega_i/W_j)}\right|_{(W_j P_1)} < \left.\frac{\partial(\sigma/A_E)_{opt}}{\partial(\omega_i/W_j)}\right|_{(\omega_i^* = W_j P_1)} \tag{55}$$

for $(\omega_i/W_j) > P_1$ and $\omega_i^* = P_1 W_j$. From equation (55), the conclusion can be drawn that the segment BC of Fig. 7 is always below Curve I.

Whenever the inequality $\omega_i > P_1 W_j$ holds, another OL with slope $P = P_2$, $P_2 > P_1$, such that $\omega_i = W_j P_2$ may be considered. This new situation corresponds to an optimal solution represented by point B′ of Fig. 7.

According to the discussion above, the following inequalities hold:

$$\left(\frac{\sigma}{A_E}\right)_{opt,B} < \left(\frac{\sigma}{A_E}\right)_C < \left(\frac{\sigma}{A_E}\right)_{opt,B'}. \tag{56}$$

Therefore, as is shown in Fig. 7, when process streams are matched according to an OL $T = P_1 t$, with $\omega_i > P_1 W_j$ and observing the constraints imposed on the model, the value of (σ/A_E) obtained (point C) is bounded 'from below' by the optimal value corresponding to P_1 (point B), and it is bounded 'from above' by the optimal value corresponding to P_2, $\omega_i = P_2 W_j$ (point B′).

These results will be used to show that thermal integration along the OL given by $T = P_1 t$ still yields the lowest value for the ratio σ/A_E for $\omega_i > P_1 W_j$, when compared on an equal exchange area basis with the solution obtained with other OLs.

This can be proven by contradiction. As an initial step, for $\omega_i/W_j > P_1$ and $\omega_i = W_j P_2$ it is assumed that there is an OL $T = f^*(t)$ different from the one given by equation (45), such that for the same value of A_E required by the solutions represented by B and C, yields a value of $(\sigma/A_E)^*$ for which the following inequalities hold:

$$\left(\frac{\sigma}{A_E}\right)_{opt,B} < \left(\frac{\sigma}{A_E}\right)^* < \left(\frac{\sigma}{A_E}\right)_C < \left(\frac{\sigma}{A_E}\right)_{opt,B'} \quad (57)$$

i.e. the solution obtained with $T = f^*(t)$ is assumed to be better than the one obtained with $T = P_1 t$, represented by C in Fig. 7. For any value of $\omega_i/W_j > P_1$, the sequence of terms in the inequalities of equation (57) must remain the same as long as functions $T = P_1 t$ and $T = f^*(t)$ are not altered.

Because $T = f^*(t)$ is not the minimal OL, when B′ approaches B by making ω_i/W_j tend to P_1 keeping both $T = P_1 t$ and $T = f^*(t)$ unchanged, also C necessarily approaches B. If the function $T = f^*(t)$ existed and since σ/A_E attains its minimum value $(\sigma/A_E)_{opt,B}$ for $T = P_1 t$, then in this operation a limiting situation should be reached in which

$$\left(\frac{\sigma}{A_E}\right)_{opt,B} < \left(\frac{\sigma}{A_E}\right)_C < \left(\frac{\sigma}{A_E}\right)_{opt,B'} < \left(\frac{\sigma}{A_E}\right)^*. \quad (58)$$

But, as was already pointed out, the sequence of these terms should have remained equal to that of equation (57), since it does not depend on the amount by which ω_i exceeds the product W_j/P_1, but solely on the functional forms of $T = P_1 t$ and $T = f^*(t)$. Therefore, if a sequence of terms like the one given by equation (58) holds in the limit $\omega_i \to W_j P_1$, it must hold for any $\omega_i > W_j P_1$. Since $f^*(t)$ is arbitrary, then the condition

$$\left(\frac{\sigma}{A_E}\right)_C < \left(\frac{\sigma}{A_E}\right)^* \quad (59)$$

guarantees that for $\omega_i > W_j P_1$ the least value of (σ/A_E) is obtained for the corresponding value of A_E by stream integration according to the OL $T = P_1 t$.

As an illustration, solutions represented by points C and B′ of Fig. 7 were obtained for the test problem given in Table 1. Table 2 shows their energy performance for $P_1 = 1.02$ and $P_2 = 1.04$, respectively. They are also compared with a 'perturbed' solution, C′, obtained from the one represented by point C of Fig. 7, by avoiding stream integration along $T = P_1 t$ in those (i, j) subregions for which $\omega_i > P_1 W_j$. In all cases ΔQ_v is the extra amount of heat to be supplied to an SA-PGC which supplements the power output of the HAPCS in cases C and B′ in order to reach the total power generated in case C′.

Table 1. Data for example problem

Process stream number and type	Supply temperature (K)	Target temperature (K)	Heat capacity flow rate (MW K^{-1})
1 (cold)	313	453	0.40
2 (hot)	573	353	0.50
3 (cold)	413	553	0.52
4 (hot)	473	313	0.45

$U = 7.5$ kW m^{-2} K^{-1}. Utilities: steam at $T_v = 650$ K, cooling water at $T_0 = 288$ K.

6.3. *Derivation of the sufficient condition*

So far, the necessary conditions for the existence of a minimal OL (or equivalently, of a weak minimum of the functional σ^*) have been derived. However, the sufficient condition for a minimum must be analyzed so as to insure that the solution found corresponds to a strong minimum of σ^*. In that sense, it can be proven that Weierstrass' condition [9], which guarantees sufficiency, is satisfied in this case. This condition establishes that, in order for the function $T(t)$ to achieve a strong minimum of the functional given by equation (34a), it is sufficient that for any T_t the inequality

$$\xi(t, T, T_t, P) = F(t, T, T_t) - F(t, T, P) - (T_t - P)\frac{\partial F}{\partial P}(t, T, P) \geqslant 0 \quad (60)$$

holds.

Substituting equations (45) and (46b) into equation (60) gives

$$\xi(t, T, T_t, P) = \left[\frac{1}{T_v} - \frac{1}{T} + \frac{\lambda}{U}\frac{1}{(T-t)}\right] \times \sum_i \sum_j \Theta_1^{(i)}(t)\Theta_2^{(j)}(T)(\omega_i - W_j T_t) \times \{\theta(W_j T_t - \omega_i + \varepsilon) - \theta(W_j P - \omega_i + \varepsilon)\}. \quad (61)$$

Since only single-value functions are acceptable as OLs, then it must hold that $T_t > 0$ for all values of t.

From equation (61) it can be seen that, whether $T_t > \omega_i/W_j$ or $0 < T_t < \omega_i/W_j$, ξ has the opposite sign to that of the expression inside the square brackets. Hence ξ will be either positive or zero in the region on the t vs T plane for which

$$\frac{1}{T_v} - \frac{1}{T} + \frac{\lambda}{U}\frac{1}{(T-t)} \leqslant 0. \quad (62a)$$

Therefore, optimal OLs are straight lines through the origin with slope given by equation (46b), lying inside the region

$$\left(\frac{T_v - T}{T_v}\right)\left(\frac{T-t}{T}\right) > \frac{\lambda}{U}. \quad (62b)$$

This region will be referred to as the optimality region.

7. DISCUSSION OF THE SOLUTION

The optimal OLs form a set of straight line segments with common intersection at the origin on a t vs T plane. Each one corresponds to a different value of λ and lies inside the optimality region given by equation (62b). The slope P of an OL in the optimal set is given by the corresponding λ value through the expression of equation (46b). As these results do not depend upon a particular set of streams, they can be presented in a problem independent chart (see Fig. 4 of Paper I).

Among all (i, j) subregions, only those encountered

Table 2. Energy performance of different solutions for the problem of Table 1

Comparison of solutions	C (refer to Fig. 7)	B′ (refer to Fig. 7)	C′ ('perturbed' solution)
P	1.02	1.04	1.02
σ_E (kW K^{-1})	5.84	11.45	4.08
σ_v (kW K^{-1})	0.39	0.29	20.13
A_E (m^2)	1986.06	992.49	1387.43
$(\sigma/A_E)\times 10^3$ (kW K^{-1} m^{-2})	3.14	11.83	17.45
Q_E (MW)	127.91	127.74	82.38
τ_{HS} (MW)	14.94	13.45	20.18
τ_{CS} (MW)	0.25	0.19	13.09
G (MW)	86.17	84.59	66.05
Q_v (MW)	1.14	1.25	59.51
ΔQ_v (MW)	32.45	35.25	—
$\eta = (\tau_{HS}+\tau_{CS}/Q_v+\Delta Q_v)$	0.99	0.91	0.56

by the optimal OL will play a part in the optimal solution. However, in order to implement heat integration along the optimal OL, the heat capacity flow rate of the thermally matched branches of the CCS and the HCS must satisfy

$$P = \frac{\omega_i}{W_j} \tag{63}$$

inside each participating (i, j) subregion. This condition can always be satisfied by splitting the stream with heat capacity flow rate in excess, giving rise to a local heat source or sink, depending on whether the split stream is hot or cold.

Figure 8 shows the optimal OL and its corresponding optimality region for a given λ/U value. Inside a participating (i, j) subregion, process streams are matched in counter-current flow pattern as it is required by equation (45).

As can be seen, the temperature difference between matched process streams is proportional to the absolute temperatures of both participating streams, as given by

$$\Delta T(t) = [P(\lambda)-1]t \tag{64a}$$

or

$$\Delta T(T) = \left[\frac{P(\lambda)-1}{P(\lambda)}\right]T \tag{64b}$$

which are two equivalent ways of expressing ΔT as a function of the temperature level.

The λ parameter plays an important role in the choice of the kind of solution wanted. In fact, a solution for which λ/U is very small will be eligible only when energy savings have an economic value that overwhelms additional capital costs. Under such circumstances, larger areas of heat exchangers can be afforded and heat exchange can be conducted closer to the equilibrium OL $T = t$, $t < T_v$. On the other hand, optimal solutions with large values of λ/U are the only eligible solutions when capital costs, related to A_E, dominate over energy (operating) costs. In the limit for $\lambda/U \to 1$, the optimality region satisfying equation (62b) collapses into the single point ($T = 0$, $t = 0$, $\lambda/U = 1$) and optimal thermal integration is not possible.

Figure 9 is a representation of the mathematical surface obtained in the t vs T vs λ/U (or equivalently t/T_v vs T/T_v vs $((\sigma^*-\sigma)/UA_E)$ space when equation

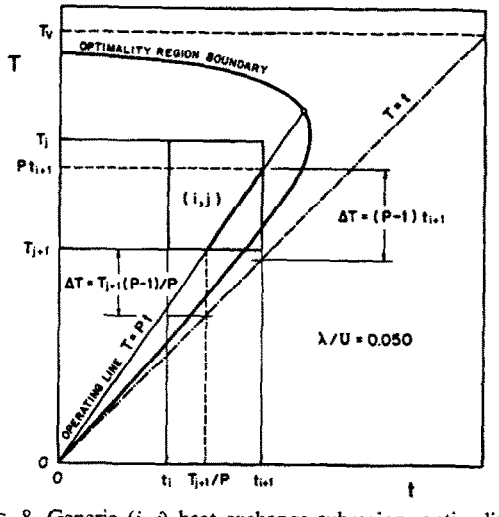

FIG. 8. Generic (i, j) heat exchange subregion, optimality region boundary and optimal OL for $\lambda/U = 0.050$.

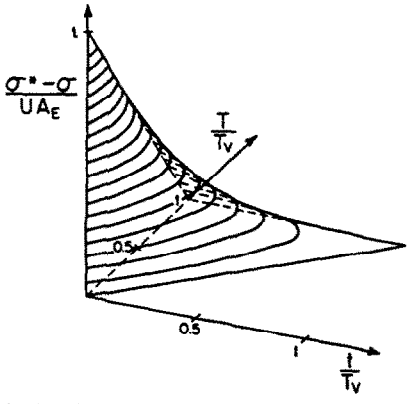

FIG. 9. Optimality surface in which the exchange region has to be included so as to insure optimality conditions.

(62b) is considered an equality. This figure illustrates the limiting situations already discussed.

Though λ/U can have any value between 0 and 1, it should be noted that in each particular problem the range of interest is restricted to those values corresponding to OLs that intersect the region on the t vs T plane that is common to the exchange region and the optimality region.

The physical meaning of the optimality region was elucidated in Paper III: inside the optimality region corresponding to a particular value of λ, further integration between the HCS and the CCS, starting from any initial degree of completion, yields an increase of G per unitary increase of A_E greater than λT_0. In any case, choosing a value of λ amounts to choosing a threshold value for the total power recovered G per unit of the total area of heat exchangers. As a consequence, $\gamma = G/A_E > \lambda T_0$ for the entire system, provided that the OL is completely included in the optimality region corresponding to λ.

In Paper III it was also shown that the lost work corresponding to an elementary heat exchange process between composite streams along an optimal OL, δLW_E, per unit heat exchange area, is given by

$$\frac{\delta LW_E}{\delta A_E} = \frac{\lambda}{1-\sqrt{\left(\frac{\lambda}{U}\right)}}. \tag{65}$$

This expression suggests the physical meaning of the optimal OL: it represents a matching policy between the HCS and the CCS leading to an HEN in which the loss of work due to heat exchange between integrated streams (or equivalently, the corresponding σ_E value) per unit A_E and unit time is a constant throughout the entire HEN, regardless of the temperature level at which the heat exchange occurs, and solely depends upon the chosen λ value.

As is shown in the calculus of variations, the multiplier λ gives the rate of change of the extreme value of the functional σ (or G) with respect to the exchange area A_E [10], given by

$$\frac{\partial \sigma}{\partial A_E} = -\lambda \tag{66a}$$

or

$$\frac{\partial G}{\partial A_E} = \lambda T_0 \tag{66b}$$

respectively.

Alternatively, it may be said that λ measures the sensitivity of σ (or G) to changes in the constraint value A_E representing the total area of heat exchangers. Then, according to equations (66) the multiplier λ gives a measure of how much the maximum profit (measured by G) or the minimum cost (measured indirectly by σ) will be changed if the exchange area changes by one unit. Hence λ can be interpreted in this case as a shadow value of shadow price per unit of A_E [10].

It is easier to carry out calculations in terms of the slope P rather than in terms of λ. This is possible due to the relationship between P and λ given by equations (46b).

Different P values will give different pairs of values of A_E and G, but each pair will correspond to the maximum ratio of $\gamma = G/A_E$ compared with other solutions with the same exchange area.

An initial choice of P can be made so as to obtain a given average ΔT value for the integrated system (i.e. $\Delta T_{average} = 10$°C), fixed on technical grounds. Then, different values of P can be scanned around the initial one, each one corresponding to optimal solutions with different A_E and G but always with the maximum in γ.

8. APPLICATION TO AN EXAMPLE

In order to show how the method is used, an optimal solution will be obtained for the problem introduced in Table 1. For illustration purposes, computations will be carried out for $P = 1.02$ ($\lambda = 0.00038$), corresponding to a logarithmic mean temperature difference of about 8.3°C.

The definition of a modified temperature, $\bar{T}$, as given by equations (31) is useful so as to work with a single temperature variable for both exchanging streams. In the OLM, this new variable can be obtained by combining equations (31) and (45) to give

$$\bar{T} = \left(\frac{P+1}{2}\right) t \tag{67a}$$

for the CCS, and

$$\bar{T} = \left(\frac{P+1}{2P}\right) T \tag{67b}$$

for the HCS.

Figure 10(a) is a schematic representation of process streams from which can be derived different temperature intervals where thermal integration must be carried out. Temperature intervals along the $\bar{T}$-axis were calculated by means of equations (67) for $P = 1.02$.

The point of intersection between the chosen optimal OL and the corresponding optimality region boundary can be obtained from equations (45) and (62b). Its coordinates are given by

$$t_{int} = T_v\left(1-\sqrt{\left(\frac{\lambda}{U}\right)}\right)^2 \tag{68a}$$

and

$$T_{int} = T_v\left(1-\sqrt{\left(\frac{\lambda}{U}\right)}\right) \tag{68b}$$

respectively, or in terms of $\bar{T}$

$$\bar{T}_{int} = \left(\frac{P+1}{2P^2}\right) T_v. \tag{68c}$$

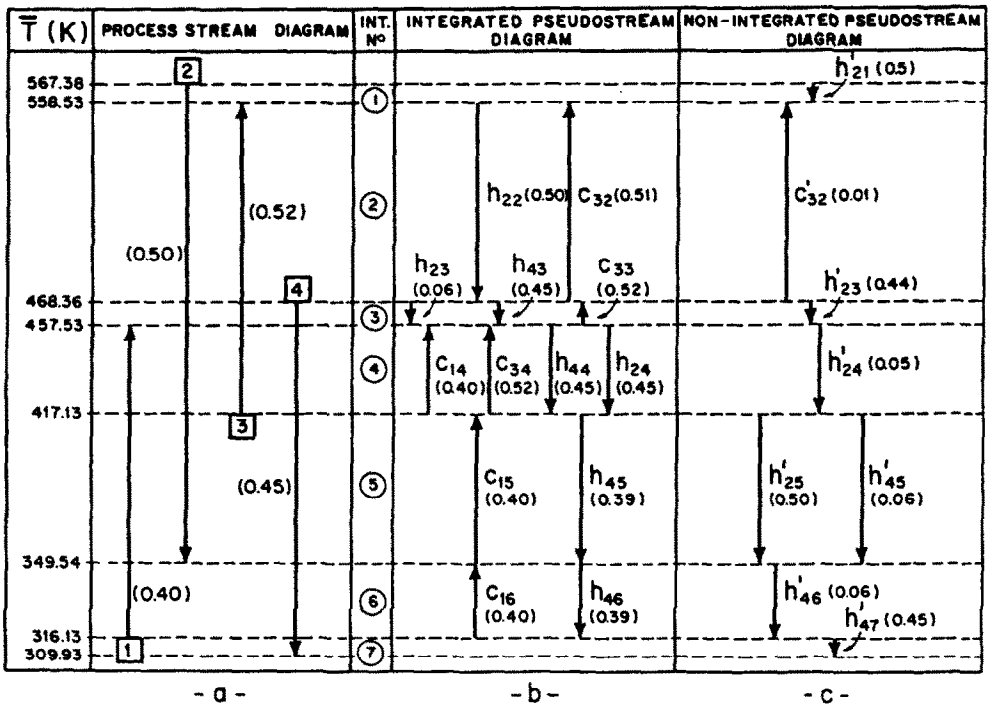

FIG. 10. Schematic representation of process streams and pseudostreams. Calculations were performed for $P = 1.02$.

In this example $\bar{T}_{int} = 631.00$ K. It is important to remark that the maximum stream temperature for this example is $\bar{T} = 567.38$ K. Hence, the exchange region is completely inside the optimality region for the chosen P value.

Stream splitting is to be performed inside each temperature interval in order to insure that the ratio cold-to-hot stream heat capacity flow rate satisfies equation (65).

The result is shown in Fig. 10(b), where c_{ij} represents the heat capacity flow rate of the cold pseudostream derived from the ith process stream in the jth temperature interval. These cold pseudostreams are to be matched against hot pseudostreams, h_{kj} in the same interval, the designation of which has an interpretation analogous to that of cold pseudostreams. For instance, in interval No. 3 the HCS heat capacity flow rate has a value such that $PW_3 > \omega_3$, for $P = 1.02$, $W_3 = 0.95$ MW K^{-1} and $\omega_3 = 0.52$ MW K^{-1}. In order to satisfy equation (65) the HCS must be split so that the heat capacity flow rate of the branch which is matched against the CCS is equal to $W_3^* = 0.51$ MW K^{-1}. In terms of original streams, HS No. 2 is bifurcated in the same interval. One of its branches, represented by pseudostream h_{23}, is matched against CS No. 3, represented by pseudostream c_{33}. The other branch, represented by pseudostream h'_{23} in Fig. 10(c), will remain as a process heat source to be coupled to a PGC. In the same interval, HS No. 4 is matched against CS No. 3.

Due to the way it was constructed, each temperature interval in Fig. 10(b) is thermally balanced. Note that, according to the definition of $\bar{T}$ given by equations (67), the absolute values of the differences between inlet and outlet temperatures of cold pseudostreams in each interval are smaller than the corresponding differences for hot pseudostreams. This explains the fact that each interval in Fig. 10(b) is energy self-sufficient although the total heat capacity flow rate of cold pseudostreams is larger than the corresponding one for hot pseudostreams.

From the results displayed in Fig. 10(b), Q_E and A_E values can be calculated in each interval and hence, the total value of Q_E and A_E for the entire system.

Figure 10(c) shows the unmatched branches of split process streams. They are designated as in the case of hot and cold pseudostreams, except that now 'primed' letters are used to distinguish them from thermally integrated pseudostreams. They represent the process heat sinks and sources remaining after stream integration has been performed according to the chosen optimal OL.

When used as a targeting procedure the OLM considers the PGCs coupled to the HEN as ideal ones. From Fig. 10(c) the maximum power that can be generated by PGCs coupled to local process heat sinks and sources can be calculated. In interval No. 3, for instance, the unmatched branch of HS No. 2 (i.e. pseudostream h'_{23}) is a local process heat source from which the maximum amount of work $\tau_{HS}^{(3)} = 1.85$ MW can be generated.

Interval No. 2 shows an energy deficit, which

appears as a cold pseudostream in Fig. 10(c). This deficit can be met by direct heating by means of the hot utility, as was assumed in the formulation of the model. When searching for the optimal solution, this assumption was only a means to penalize the use of high quality energy for direct or indirect heating purposes over its use to generate shaft power in an SA-PGC of higher efficiency.

When the optimal solution is implemented for a particular problem, this constraint is relaxed by using PGCs that discharge heat to every local process sink, producing an extra amount of shaft power τ_{CS}. This evolution neither changes the value of the objective function nor modifies the optimal OL, so that the optimum reached remains unchanged. When this is done for interval No. 2, a contribution of $\tau_{CS}^{(2)} = 0.252$ MW to the total amount of power generated is obtained.

The energy performance of the optimal solution for $P = 1.02$ is shown in Table 2 as solution C.

When this procedure is repeated for several P values a set of optimal solutions (each one corresponding to different A_E and G/A_E values) can be obtained. The final choice of the most profitable solution among this set of energy optimal solutions can be made on the basis of additional economic arguments, that are beyond the scope of this paper.

The optimal HEN for the chosen optimal solution can be derived with the of the h_{ij}/c_{kl}-tableau and can be represented in the 'grid' form [11]. For more details, the reader is referred to Paper II.

9. CONCLUSIONS

The physical and mathematical models on which the OLM are based have been presented together with a thorough discussion of the mathematical technique used to tackle the optimization problem.

The results obtained through a rigorous mathematical procedure are condensed in simple, well-established mathematical expressions that can be easily implemented to solve each particular optimal synthesis problem. The final, explicit relationships between operational and design parameters that characterize the optimum can be incorporated to the designer's background enabling him to understand the 'physiology' of the optimal solution and to anticipate the impact of technical decisions.

Acknowledgements—The authors would like to acknowledge the financial support provided by the Universidad Nacional del Litoral and by the Consejo Nacional de Investigaciones Cientificas y Técnicas (CONICET), Argentina.

REFERENCES

1. H. A. Irazoqui, Optimal thermodynamic synthesis of thermal energy recovery systems, *Chem. Engng Sci.* **41**, 1243–1255 (1986).
2. P. A. Aguirre, E. O. Pavani and H. A. Irazoqui, Comparative analysis of pinch and operating line method for heat and power integration, *Chem. Engng Sci.* **44**, 803–816 (1989).
3. P. A. Aguirre, E. O. Pavani and H. A. Irazoqui, Optimal synthesis of heat-and-power systems with multiple steam levels, *Chem. Engng Sci.* **45**, 117–129 (1990).
4. D. W. Townsend and B. Linnhoff, Heat and power networks in process design (I), *A.I.Ch.E. Jl* **29**, 742–748 (1983).
5. I. Prigogine and R. Defay, *Chemical Thermodynamics* (5th Edn), p. 34. Longmans, London (1969).
6. O. Bolza, *Lectures on the Calculus of Variations* (3rd Edn). Chelsea, New York (1973).
7. M. J. Lighthill, *Introduction to Fourier Analysis and Generalised Functions* (9th Edn), p. 30. Cambridge University Press, Cambridge (1980).
8. B. Linnhoff, D. W. Townsend, D. Boland, G. F. Hewitt, B. E. A. Thomas, A. R. Guy and R. H. Marsland, *A User Guide on Process Integration for the Efficient Use of Energy*, p. 20. The Institution of Chemical Engineers, Rugby (1982).
9. Iu. P. Petrov, *Variational Methods in Optimum Control Theory*, p. 93. Academic Press, New York (1968).
10. D. R. Smith, *Variational Methods in Optimization*, p. 92. Prentice-Hall, Englewood Cliffs, New Jersey (1974).
11. J. Cerdá and A. W. Westerberg, Synthesizing heat exchanger networks having restricted stream/stream matches using transportation problem formulations, *Chem. Engng Sci.* **38**, 1723–1740 (1983).

APPENDIX

Operating on equation (34b), it results

$$F_T(t, T, T_i) = \Phi_{ij}(T_i)\left[\frac{1}{T^2} - \frac{\lambda}{U}\frac{1}{(T-t)^2}\right] \quad \text{(A1)}$$

and

$$F_{T_i}(t, T, T_i) = \Phi'_{ij}(T_i)\left[\frac{1}{T_v} - \frac{1}{T} + \frac{\lambda}{U}\frac{1}{(T-t)}\right] \quad \text{(A2)}$$

which are the expressions of the derivative appearing in equation (40a), obtained after the generalized function R has been substituted by its definition as given by equations (19).

Since the solution sought belongs to the class represented by equations (41), with piece-wise constant slope, equations (A1) and (A2) become

$$F_T(t, T, P_{ij}) = \Phi_{ij}(P_{ij})\left[\frac{1}{T^2} - \frac{\lambda}{U}\frac{1}{(T-t)^2}\right] \quad \text{(A3)}$$

and

$$F_{T_i}(t, T, P_{ij}) = W_j \times \text{sign}\,(P_{ij}) \times [1-\theta(W_j|P_{ij}|-\omega_i+\varepsilon)] \times \left[\frac{1}{T_v} - \frac{1}{T} + \frac{\lambda}{U}\frac{1}{T-t}\right] \quad \text{(A4)}$$

respectively.

The total derivative in the second term of equation (40a) is

$$\frac{d}{dt}F_{T_i}(t, T, P_{ij}) = W_j \times \text{sign}\,(P_{ij}) \times [1-\theta(W_j|P_{ij}|-\omega_i+\varepsilon)] \times \left[\frac{P_{ij}}{T^2} - \frac{\lambda}{U}\frac{(P_{ij}-1)}{(T-t)^2}\right] \quad \text{(A5)}$$

where advantage has been taken of the fact that $T_i = P_{ij}$ inside the (i, j) subregion, with P_{ij} a constant value.

Substituting equations (A3) and (A5) into equation (40a), and taking into account that

$$\text{sign}\,(P_{ij})P_{ij} = |P_{ij}|$$

the expression given by equation (42) can be readily obtained.

SYNTHESE OPTIMALE DES SYSTEMES ENERGETIQUES: LA METHODE DE LA LIGNE OPERATOIRE

Résumé—Les modèles physique et mathématique sur lesquels est construite la méthode de la ligne opératoire (OLM) (H. A. Irazoqui, *Chem. Engng Sci.* **41**, 1243–1255 (1986); P. A. Aguirre, E. O. Pavani et H. A. Irazoqui, *Chem. Engng Sci.* **44**, 803–816 (1989)), pour la synthèse optimale des systèmes énergétiques, sont discutés en profondeur. Ces modèles incluent les "modes" d'échange de chaleur de façon à obtenir un schéma optimal pour les systèmes d'énergie totale dans les usines chimiques. On fait aussi un développement de la technique mathématique utilisée pour traiter le problème d'optimisation. Ce développement comprend la dérivation des conditions nécessaires et suffisantes de l'optimalité.

OPTIMALE SYNTHESE VON WÄRME-KRAFT-SYSTEMEN: DAS VERFAHREN DER BETRIEBSKENNLINIEN

Zusammenfassung—Die physikalischen und mathematischen Modelle, auf denen das Verfahren der Betriebskennlinie (H. A. Irazoqui, *Chem. Engng Sci.* **41**, 1243–1255 (1986); P. A. Aguirre, E. O. Pavani und H. A. Irazoqui, *Chem. Engng Sci.* **44**, 803–816 (1989)) für eine optimale Synthese von Wärme-Kraft-Systemen beruht, werden eingehend diskutiert. Diese Modelle enthalten die zugelassenen Formen von Wärmeübertragung und die allgemeinen Besonderheiten der Lösung, die gesucht wird um eine optimale Anordnung des gesamten Energiesystems in chemischen Werksanlagen zu erlangen. Die erforderlichen mathematischen Verfahren zur Behandlung des Optimierungsproblems werden durchgehend entwickelt. Diese Entwicklung enthält die Herleitung der notwendigen und hinreichenden Bedingungen für einen optimalen Zustand.

ОПТИМАЛЬНЫЙ СИНТЕЗ ТЕПЛОВЫХ И ЭНЕРГЕТИЧЕСКИХ СИСТЕМ: МЕТОД РАБОЧИХ КРИВЫХ

Аннотация—Обсуждаются физические и математические модели, на основе которых разработан метод рабочих кривых (OLM) (H. A. Irazoqui, *Chem. Engng Sci.* **41**, 1243–1255 (1986); P. A. Aguirre, E. O. Pavani and H. A. Irazoqui, *Chem. Engng Sci.* **44**, 803–816 (1989)) для оптимального синтеза тепловых и энергетических систем. Эти модели включают допустимые режимы теплообмена и общие характеристики вида искомого решения для разработки оптимальной схемы энергетических систем в химических производствах. Разработаны математические методы решения задачи, определены необходимые и достаточные условия оптимизации.